Chemical Engineering Journal 162 (2010) 710–717

Contents lists available at ScienceDirect

Chemical Engineering Journal

journal homepage: www.elsevier.com/locate/cej

Preparation of nitrogen and fluorine co-doped mesoporous TiO_2 microsphere and photodegradation of acid orange 7 under visible light

Yongmei Wu [a], Mingyang Xing [a], Baozhu Tian [a], Jinlong Zhang [a,b,*], Feng Chen [a]

[a] Key Laboratory for Advanced Materials and Institute of Fine Chemicals, East China University of Science and Technology, 130 Meilong Road, Shanghai 200237, PR China
[b] School of Chemistry and Materials Science, Guizhou Normal University, Guiyang 550001, PR China

ARTICLE INFO

Article history:
Received 2 April 2010
Received in revised form 19 June 2010
Accepted 23 June 2010

Keywords:
Titania miscrosphere
Nitrogen and fluorine codoping
Photocatalysis
Visible light

ABSTRACT

N and F-codoped TiO_2 microspheres were prepared by ethanol solvothermal method, using tetrabutyl titanate as precursor, urea as a nitrogen source and ammonium fluoride as a fluorine source. The prepared catalysts were characterized by X-ray diffraction (XRD), N_2 physical adsorption, scanning electron microscopy (SEM), X-ray photoelectron spectroscopy (XPS), ultraviolet–visible adsorption spectroscopy and photoluminescence spectra (PL). The photocatalytic performance of N–F–TiO_2 microspheres was evaluated by analyzing the degradation of acid orange 7 (AO7) under visible light irradiation. It was found that N–F–TiO_2 microsphere with mesoporous structure is composed by anatase phase, and the interstitial doping of nitrogen into TiO_2 lattice might be responsible for the visible light response. Meanwhile, F-doping could not only retard the transformation from anatase to rutile, but also increase the concentration of $OH^{\bullet}$ radicals in solution, which is beneficial for improving the photodegradation rate of organic compounds. The synergetic effect of nitrogen and fluorine doping leads to the high activity of N–F–TiO_2 for the photodegradation of AO7 under visible light irradiation.

1. Introduction

As one of the most promising photocatalysts, nanosized TiO_2 has long been investigated for photocatalytic degradation of organic pollutants, photocatalytic dissociation of water, solar energy conversion and disinfection [1–3]. However, its band gap (3.2 eV for anatase) is so wide that only ultraviolet (UV) light can be absorbed. A promising approach to achieve the visible light activity of TiO_2 is doping TiO_2 with a non-metal element, such as N, C, S, B, and F [4–8]. Among them, the N-doped TiO_2 seems to be the most efficient and the most extensively investigated. N-doped TiO_2 photocatalysts have been prepared by high temperature sintering of TiO_2 under N-containing atmosphere [4,9,10], sputtering, implantation [11,12], and wet chemical method such as sol–gel, hydrothermal treatment in the presence of N-precursor containing ammonia or organic amines [13–15]. Nakamura et al. [10] proposed that the visible light response for N-doped TiO_2 arises from an N-induced mid-gap (N 2p) level, formed slightly above the top of the (O 2p) valence band. Asahi et al. [4] theoretically calculated the band structure of the N-doped TiO_2 and concluded that the visible light sensitivity is due to the narrowing of the band gap by mixing the N 2p and O 2p states. The origin of visible light photoactivity of N-doped TiO_2 is still in debate. Yu et al. demonstrated F-doping into TiO_2 can induce visible light-driven photocatalytic activity for degradation of gas-phase acetone [8]. Compared with single non-metal dopant, doping two kinds of non-metal atoms such as S and N atoms [16,17], C and N atoms [18,19], B and N [20,21] and F and N atoms [22–27] has shown more beneficial effects. Li et al. [22,23] synthesized N and F-codoped TiO_2 spheres from a mixed aqueous solution containing $TiCl_4$ and NH_4F by spray pyrolysis and the as-prepared N–F–TiO_2 exhibited higher visible light activity than N-doped or F-doped TiO_2, because the doped N atoms improved the visible light absorption and the doped F atoms enhanced the surface acidity and the adsorption of agents. Huang et al. [24] prepared N and F-codoped TiO_2 by a sol–gel-solvothermal method using triethylamine as a nitrogen source, and ammonium fluoride as a fluorine source and the N–F-codoped TiO_2 powder showed high photocatalytic activity for *p*-chlorophenol and Rhodamine B under visible light irradiation. Xie et al. [25] reported F–N-comodified TiO_2 photocatalysts prepared at low temperature using $TiCl_4$ as precursor, ammonia as nitrogen source and ammonium fluoride as fluorine source, which also exhibited good photoactivity for degradation of methyl orange under visible light. Livraghi et al. [26] prepared N–F-codoped TiO_2 using ammonium fluoride as source of dopants by sol–gel synthesis and successive calcinations in air. Di Valentin et al. [27] investigated N–F-codoped TiO_2 through a com-

* Corresponding author at: Key Laboratory for Advanced Materials and Institute of Fine Chemicals, East China University of Science and Technology, 130 Meilong Road, Shanghai 200237, PR China. Tel.: +86 21 64252062; fax: +86 21 64252062.
E-mail address: jlzhang@ecust.edu.cn (J. Zhang).

1385-8947/$ – see front matter © 2010 Elsevier B.V. All rights reserved.
doi:10.1016/j.cej.2010.06.030

bined theoretical and experimental study. Their experiment results confirmed that the incorporation of nitrogen was favored in the presence of fluorine and the photocatalytic activities of N–F–TiO_2 under visible light irradiation were enhanced compared with the single doped materials. However, among these N–F–TiO_2 photocatalysts reported in the literature, only N–F-codoped TiO_2 by spray pyrolysis under high temperature consisted of spherical particles, synthesis of mesoporous N–F-codoped TiO_2 microsphere with wet chemical method has seldom been investigated up to now.

Herein, we reported a simple one-step and template-free solvothermal method to synthesize mesoporous N and F-codoped TiO_2 microsphere using urea as a nitrogen source and ammonium fluoride as a fluorine source. In this study, the degradation of AO7 in visible light was selected as a probe reaction to measure the photocatalytic activity of different samples. It was found that the resulting N–F-codoped TiO_2 microsphere by this method exhibited much higher photoactivity than undoped TiO_2 and mono N or F-doped TiO_2.

2. Materials and methods

2.1. Catalyst preparation

The fluorine and nitrogen codoped TiO_2 sample were prepared by combining sol–gel method followed by solvothermal treatment. Tetrabutyl titanate was used as a starting material, urea as a nitrogen source, and ammonium fluoride as a fluorine source. All chemicals used in the experiments were analytical reagent grade. 3 mL tetrabutyl titanate was dissolved into 16 mL anhydrous ethanol and 0.2 mL concentrated nitric acid (68%) (solution A), urea (N/Ti = 2 mol ratio), NH_4F (F/Ti = 0.1 mol ratio) and 1 mL distilled water were dissolved into 35 mL anhydrous ethanol (solution B). Then, solution A was added drop-wise to solution B under magnetic stirring. The resultant mixture was stirred at room temperature for 2 h and then transferred into a 100 mL teflon-inner-liner stainless steel autoclave. The autoclave was kept for 16 h under 150 °C for crystallization. After this solvothermal treatment, the precipitate gained was washed by distilled water, dried at 100 °C for 24 h and calcined at 400 °C for 2 h in the muffle oven. The obtained photocatalyst was denoted as N–F–TiO_2. For comparison, the undoped TiO_2 was prepared by the similar method in the absence of urea and ammonium fluoride. F–TiO_2 was prepared in the presence of sodium fluoride and N–TiO_2 was prepared in the presence of urea.

2.2. Catalyst characterization

XRD analysis of the as-prepared photocatalysts was carried out at room temperature with a Rigaku D/max 2550 VB/PC apparatus using Cu Kα radiation (λ = 1.5406 Å) and a graphite monochromator, operated at 40 kV and 30 mA. Diffraction patterns were recorded in the angular range of 10–80° with a stepwidth of 0.02 s^{-1}. To analyze the light absorption of the photocatalysts, UV–vis absorption spectra were obtained using a scan UV–vis spectrophotometer (Varian Cary 500) equipped with an integrating sphere assembly, while $BaSO_4$ was used as a reference. To investigate the chemical states of the photocatalysts, X-ray photoelectron spectroscopy (XPS) was recorded on a Perkin Elmer PHI 5000C ESCA System with Al Kα radiation operated at 250 W. The shift of binding energy due to relative surface charging was corrected using the C 1s level at 284.6 eV as an internal standard. The porous texture of the powders was analyzed from nitrogen adsorption–desorption isotherms at 77 K. Using a Micromeritics ASAP 2000 system, the BET and BJH methods were applied for the determination of the specific surface area, and the mean mesopore equivalent diameter, respectively. The recombination of electron–hole in the samples was studied by the photoluminescence (PL) emission spectra, which was measured on a luminescence spectrometry (Cary Eclips) at room temperature under the excitation light at 280 nm.

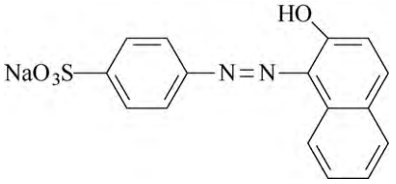

Scheme 1. Molecular structure of orange acid 7.

OH• radicals generated on the photocatalysts surface under visible light irradiation were investigated using a fluorescence spectrophotometer. About 0.15 g of the photocatalyst was added to 40 mL of terephthalic acid solution with a concentration of 0.83 g/L. The OH• radicals generated by means of visible light irradiation reacted with terephthalic acid to produce high fluorescence hydroxyterephthalic acid. The amount of 2-hydroxyterephthalic acid corresponded to the amount of OH• radicals [28]. The 2-hydroxyterephthalic acid is the only product with any significant fluorescence. The shapes of the spectra characteristic to the reaction product and wavelength of maximum emission were the same, whereas only the intensity of these spectra was changed. To determine the amount of OH• radicals, the peak areas were calculated.

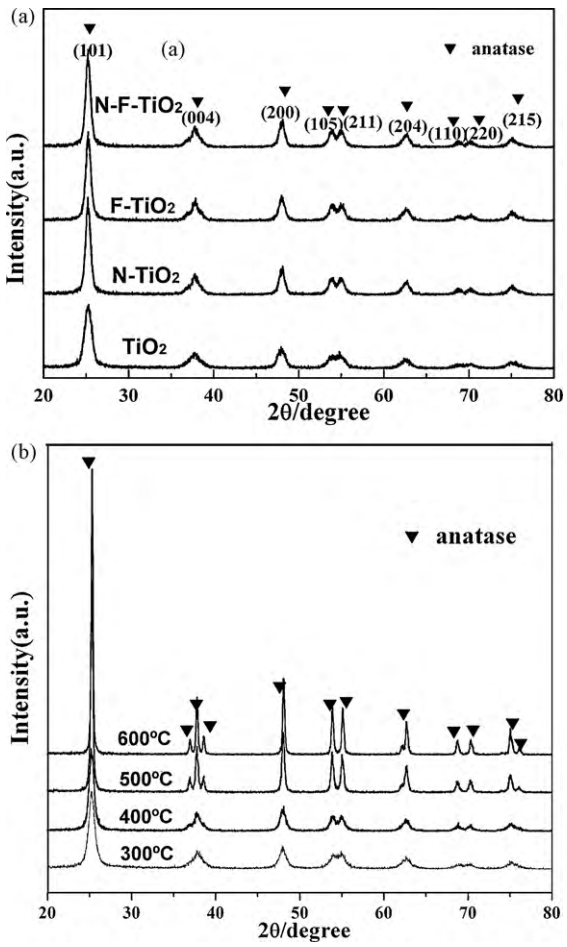

Fig. 1. XRD patterns of different samples: (a) TiO_2, N–TiO_2, F–TiO_2, and N–F–TiO_2; (b) N–F–TiO_2 samples calcined at 300, 400, 500 and 600 °C.

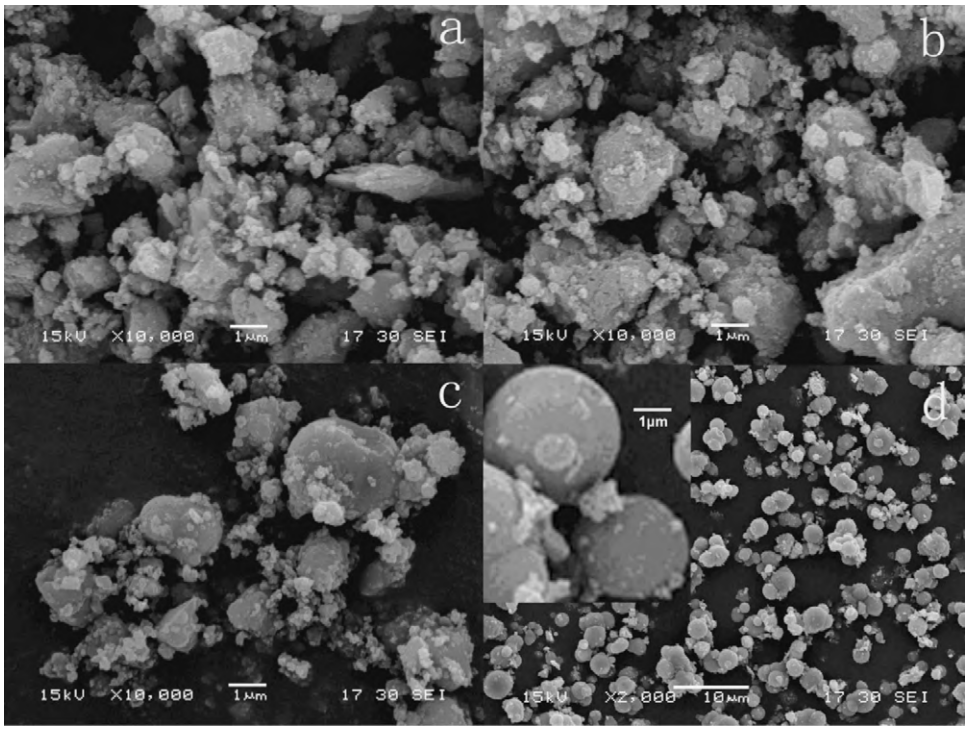

Fig. 2. SEM images of samples of (a) TiO_2; (b) F–TiO_2; (c) N–TiO_2; (d) N–F–TiO_2.

2.3. Photocatalytic activity test

The photocatalytic activities of samples were evaluated in terms of the degradation of acid orange 7 (AO7) under visible light illumination. AO7 is an azo-dyes (Scheme 1), which is difficult to decolorize and frequently-used in textile industry. The photocatalyst powder (0.08 g) was dispersed in a 100 mL quartz photoreactor containing 80 mL of a 50 mg L^{-1} AO7 solution. The mixture was sonicated for 10 min and stirred for 30 min in the dark in order to reach the adsorption–desorption equilibrium. A 1000 W tungsten halogen lamp equipped with a UV cut-off filters ($\lambda > 420$ nm) was used as a visible light source (the average light intensity was 60 mW cm^{-2}). The lamp was cooled with flowing water in a quartz cylindrical jacket around the lamp, and ambient temperature is maintained during the photocatalytic reaction. At the given time intervals, the analytical samples were taken from the mixture and immediately centrifuged, then filtered through a 0.22 μm Millipore filter to remove photocatalysts. The concentration of the filtrate was analyzed by checking the absorbance at 484 nm with a UV–vis spectrophotometer (Varian). The reproducibility was checked by repeating the measurements at least three times and was found to be within the acceptable limit (±5%).

3. Results and discussion

3.1. XRD analysis

Fig. 1a shows the XRD patterns of all of samples calcined at 400 °C. All of samples consist of anatase as a unique phase [JCPDS no. 21-1272, space group: I41/amd (141)]. Calculated from the full width half maximum (FWHM) of anatase (1 0 1) diffraction, the crystallize sizes of TiO_2, N–TiO_2, F–TiO_2, and N–F–TiO_2 are 13.5, 12.5, 13.3, and 12.9 nm, respectively. Compared to undoped TiO_2, the crystallize size of N–TiO_2, F–TiO_2 and N–F–TiO_2 slightly decreased, which indicated that non-metal doping could slightly restrain the growth of TiO_2 crystallite, similar to the previous report [23].

Fig. 1b shows the effects of calcination temperature on phase structures of N–F–TiO_2 powders. Clearly, N–F–TiO_2 powders contain only anatase phase over the calcination temperature range of 300–600 °C. Additionally, the peak intensity of anatase increases with increasing calcination temperature and the width of the (1 0 1) plane diffraction peak of anatase ($2\theta = 25.4°$) becomes narrower, suggesting that crystalline size and the relative crystallinity significantly increase. However, the rutile phase for undoped TiO_2 starts to appear at 600 °C (not shown). Hence, it could be concluded that N and F-doping suppress phase transformation from anatase to rutile. Li and co-workers [25] also found that the as-sprayed N–F–TiO_2 samples belonged to anatase when the spray pyrolysis temperature ranged from 600 to 1000 °C.

3.2. SEM images

Fig. 2 presents SEM images of undoped TiO_2, F–TiO_2, N–TiO_2 and N–F–TiO_2 calcined at 400 °C. It is found that TiO_2, F–TiO_2 and N–TiO_2 are rough and irregularly agglomerated by primary particles. However, N–F–TiO_2 consists of solid microspheres with relatively smooth surface. Their diameters are in the range of several hundred nanometers to several micrometers. The microspheres synthesized show no agglomeration and do not collapse even after calcination at 400 °C for 2 h. This result indicates that the additive of urea and ammonia fluoride is essential for the formation of N–F–TiO_2 microspheres. During the solvothermal treatment, urea would be gradually decomposed into ammonia and carbonate ions, which lead to the slow rise of the pH in the solution. Thus, the alcoholysis process of tetrabutyl titanate was initiated. While, the presence of ammonia fluoride could behave as an electrolyte and thus modify the Zeta potential of spherical poly-condensed titania species generated at the initial stage of the alcoholysis reaction [29]. The molar ratio of urea to ammonia fluoride would affect the

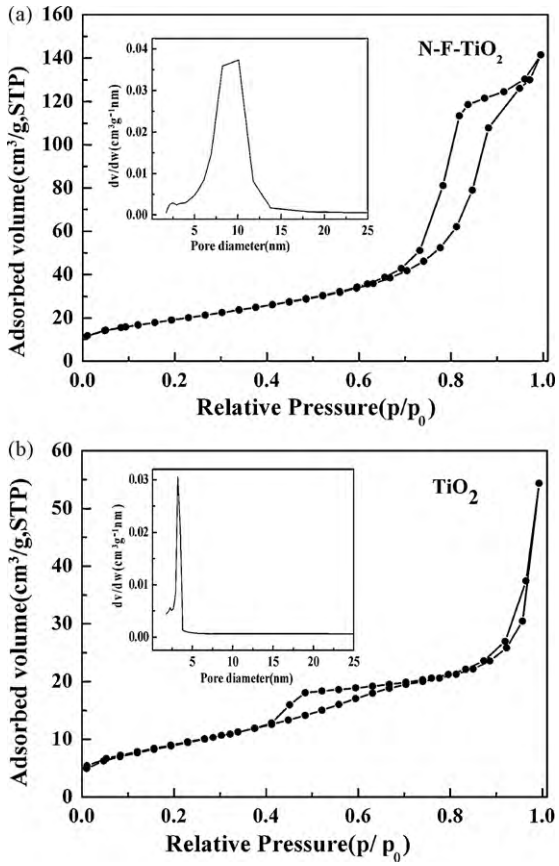

Fig. 3. N_2 adsorption–desorption isotherm of N–F–TiO_2 (a) and undoped TiO_2 (b). The inset shows their BJH pore size distribution curve.

average diameter of the N–F–TiO_2 microspheres. The investigation on this facet is in progress.

3.3. Nitrogen physical adsorption

The surface area and porosity distribution of N–F–TiO_2 microspheres and undoped TiO_2 sample calcined at 400 °C were investigated using nitrogen adsorption and desorption isotherms (shown in Fig. 3a and b). The isotherms of N–F–TiO_2 sample are typical type IV-like with a type H2 hysteretic loop, which indicates the presence of mesoporous materials according to IUPAC classification [30]. The plot of the pore size distribution (inset in Fig. 3a) was determined by using the Barrett–Joyner–Halenda (BJH) method from the desorption branch of the isotherm; it shows that N–F–TiO_2 microspheres clearly have mesoporous structure. The average pore diameter of N–F–TiO_2 microspheres is about 10 nm and the BET surface area is 78 $m^2\ g^{-1}$. Mesoporous structure is probably formed by agglomeration of primary particles (interparticle pores). However, compared to N–F–TiO_2 sample, the area of the hysteresis loop of undoped TiO_2 significantly decreases, its average pore diameter is only 2.5 nm (shown in Fig. 3b) and the BET surface area is about 36 $m^2\ g^{-1}$.

3.4. UV–vis spectra

The UV–vis absorption spectra of undoped TiO_2, F–TiO_2, N–TiO_2 and N–F–TiO_2 are shown in Fig. 4. The band gap energies can be calculated by a plot $(\alpha h\nu)^{1/2}$ versus photon energy ($h\nu$). The absorption coefficient α and indirect band gap Eg are related through the

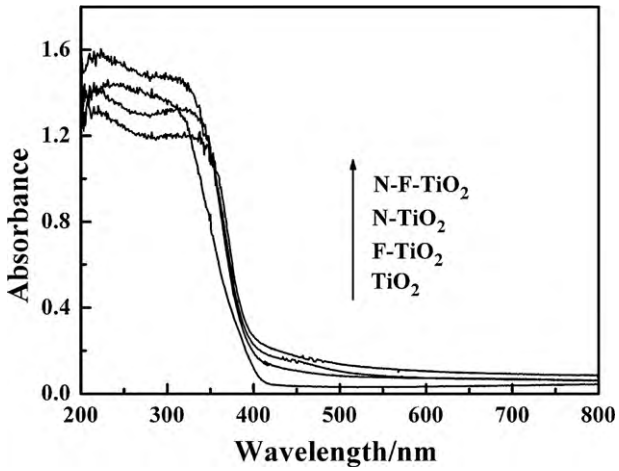

Fig. 4. UV–vis absorption spectra of different samples.

following equation [31]

$$(\alpha h\nu)^{1/2} \propto h\nu - Eg \quad (1)$$

where ν is the frequency and h is Planck's constant. The obtained energy band gaps for undoped TiO_2, F–TiO_2, N–TiO_2 and N–F–TiO_2 were 3.02, 2.95, 2.80 and 2.74 eV, corresponding to the band gap absorption onsets of 400, 421, 443 and 452 nm, respectively. Obviously, the optical absorption edges of those non-metal doped samples shift to the lower energy region compared to the undoped TiO_2. N–TiO_2 sample presents a significant absorption in the visible region, which is similar to those reported in the literature for N-doped TiO_2 [4,9,10]. This absorption in the visible region is associated to the impurity states deriving from nitrogen insertion in the bulk of the oxide. The red shift of absorption bands in the visible spectral range for F-doped TiO_2 remains under debate. Yamaki et al. [32] and Li et al. [22] found that only F-doping did not cause the red shift of absorption of TiO_2. They assumed that the F 2p states located below the bottom of the O 2p valence band, so F-doping did not affect the optical absorption property of TiO_2. But some of studies revealed that intrinsic defects, including those defects associated with oxygen vacancies, contribute to the absorption of light in the visible spectral region [33,34]. A recent study by Kuznetsov and Serpone has proposed that the commonality in these anion doped titania rests with the formation of oxygen vacancies and the advent of color centers that absorb the visible light radiation [35,36]. Some reports have confirmed that F-doping favors formation of oxygen vacancies [8,27]. So we proposed that the red shift of F–TiO_2 is contributed to oxygen vacancy. Both nitrogen and fluorine codoping can evidently narrow the band gap of TiO_2, which may be assigned to the synergistic effect of nitrogen and fluorine codoping.

3.5. XPS analysis

Fig. 5a shows the F 1s XPS spectra of the F–TiO_2 and N–F–TiO_2 samples. The F 1s region is composed of two peaks. The peak at 683.7–684.6 eV could be assigned to F^- ions physically adsorbed on the surface of TiO_2 [8]. Another small peak at 688.0–688.6 eV could be attributed to the substitutional F atoms that occupied oxygen sites in the TiO_2 crystal lattice and form bond of Ti–O–F [8,22]. Based on XPS results, the content of F atoms are 2.0% for F–TiO_2 and 1.9% for N–F–TiO_2. Additionally, it is worth to note that most of the F atoms in the F–TiO_2 and N–F–TiO_2 samples are present mainly in the form of F^- ions adsorbed on the surface of samples, while only low amount of F atoms can be incorporated into the lattice of TiO_2.

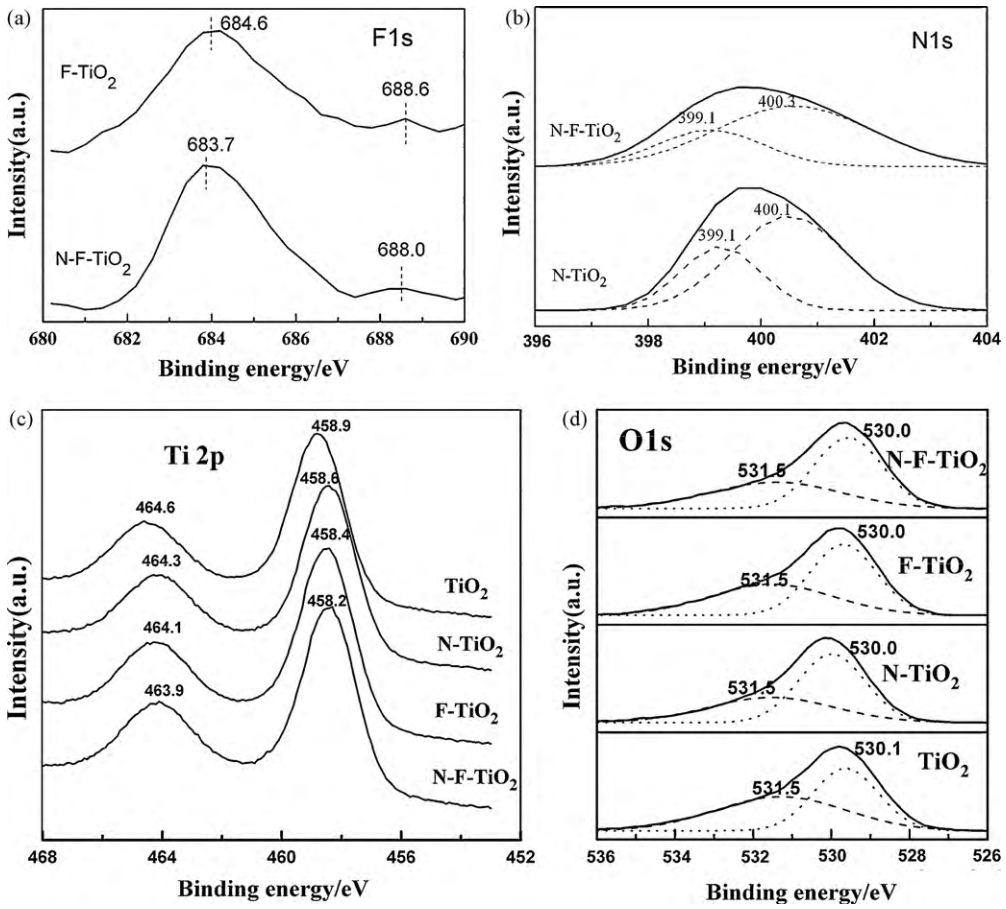

Fig. 5. XPS spectra of (a) F 1s of N–F–TiO_2 and F–TiO_2, (b) N 1s of N–F–TiO_2 and N–TiO_2, (c) Ti 2p of different samples, and (d) O 1s of different samples.

Fig. 5b shows the XPS spectra for the N 1s region of N–TiO_2 and N–F–TiO_2 samples and their fitting curves. A broad peak extending from 396 to 404 eV is observed for both of N–TiO_2 and N–F–TiO_2 samples, which is typical of nitrogen-doped titanium dioxide, reported by several other researchers [4,14]. After fitting of the curve, two peaks are obtained at 399.1 and 400.1–400.3 eV, respectively. In many cases, the peak at about 399 eV is attributed to the anionic N– in O–Ti–N linkages, in consistent with some literature proposal [14,37]. The origin of another peak above 400 eV is subject to much controversy. Asahi et al. [4] and Kisch and co-workers [14] attribute the binding energy of N 1s peaks between 400 and 402 eV to molecularly adsorbed nitrogen species. Burda and co-worker [38] suggested that it was attributed to the N atom in the environment of O–Ti–N. This peak was assigned to the formation of the Ti–O–N structure [15]. The N content was 0.78% for N–TiO_2 and 0.57% for N–F–TiO_2. Livraghi reported that F^- ions substitute oxygen in the lattice of TiO_2 favor N species incorporation in the TiO_2 and lead to higher N content than only N–TiO_2 [26]. Unfortunately, our result shows that there is similar N content between N–TiO_2 and N–F–TiO_2 samples, which may be due to the different preparation procedure.

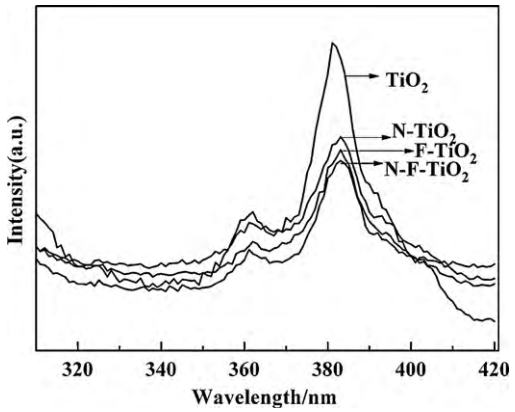

Fig. 6. Photoluminescence spectra of different samples.

Fig. 5c shows the XPS spectra for the Ti 2p region of TiO_2, F–TiO_2, N–TiO_2 and N–F–TiO_2 samples. The Ti $2p_{3/2}$ and Ti $2p_{1/2}$ of undoped TiO_2 appear at 458.8 and 464.6 eV, respectively, indicating that Ti exists in the Ti^{4+} form [39]. The binding energy of Ti 2p for F–TiO_2 decreases 0.3 eV compared to undoped TiO_2. It was reported that F-doping may convert some Ti^{4+} to Ti^{3+} by charge compensation, thus lowing the binding energy of Ti–O–Ti, the equation is shown as follow [8]:

$$TiO_2 + qF^- \rightarrow {Ti_q}^{3+}{Ti^{4+}}_{1-q}{O^{2-}}_{2-q}{F_q}^- + qO^- \quad (2)$$

But in our XPS result there is no evidence of Ti^{3+} formation. It may be attributed to lower amount of Ti^{3+} beyond the limitation of XPS detection. Meanwhile, the binding energy of Ti 2p for N–TiO_2 lower 0.5 eV than that of undoped TiO_2 suggests different electronic interactions of Ti with N anions, which causes partial electron transformation from the N atom to the Ti atom and an increase of the electron density on Ti because of the lower electronegativity of nitrogen compared to oxygen [15]. In the case of N–F–TiO_2, the binding energy of Ti 2p negatively shifts 0.7 eV, implying that some charges from nitrogen species may be transferred to Ti on the surface of TiO_2 as well as the formation of Ti^{3+}, thus leading to

increasing of charge density of Ti species. Fig. 5d shows XPS spectra for the O 1s region for these four samples. The O 1s region is composed of two peaks. One peak at 530.0 eV is attributed to the Ti–O in TiO_2 and the composite, while the other one at 531.5 eV is assigned to the hydroxyl group. N and F-doping did not cause significantly changes among these samples.

3.6. PL analysis

PL emission spectra have been widely used to investigate the efficiency of charge carrier trapping, migration, and transfer and to understand the fate of electron–hole pairs in semiconductor particles. It is known that the PL emission is resulted from the recombination of excited electrons and holes, the lower PL intensity may indicate the lower recombination rate of electron–holes under light irradiation [40]. Fig. 6 shows the PL spectra of undoped TiO_2, F–TiO_2, N–TiO_2 and N–F–TiO_2 samples. Two peaks appearing at about 360 and 380 nm are ascribed to the emission of the band gap transition [40]. It can be seen that undoped TiO_2 has the highest intensity among these samples, implying the fastest recombination rate of electron–holes. After N and F introduced into TiO_2, the PL intensity of F–TiO_2, N–TiO_2 and N–F–TiO_2 samples decreased. This result indicates the recombination of charge carriers is effectively suppressed. It was reported that doped F atoms into TiO_2 can convert Ti^{4+} to Ti^{3+} by charge compensation and that the existence of a certain amount of Ti^{3+} can reduce the electron–hole recombination rate [8,27]. In our previous study, we found the doping of nitrogen into TiO_2 lattice led to the efficient quenching of the photoluminescence [15]. The effective quenching of the photoluminescence can be attributed to the two reasons. One is the electron is trapped by the oxygen vacancy which induced by N doping, while the hole is trapped by the doped nitrogen. Another is that the excited electron can transfer from the valance band to the new levels that exist upper of the conduction band introduced by nitrogen doping, which can also decrease the photoluminescence intensity. Therefore, a synergistic effect of N and F codoping would lead to improving the electron–hole separation.

3.7. Photocatalytic activities

Fig. 7a shows the visible light-induced photocatalytic decomposition of AO7 with N–F-codoped TiO_2 photocatalysts. It can be seen that no degradation of AO7 takes place in the absence of photocatalyst. The degradation rate of AO7 on the P25 and undoped TiO_2 under visible light irradiation is very low, which can be attributed to the self-sensitization of AO7. Among them, the N–F-codoped TiO_2 shows the highest photodegradation activity, which is four and three times higher than that by commercial P25 TiO_2 and undoped TiO_2, respectively. Additionally, F–TiO_2 also exhibits higher photoactivity than N–TiO_2, although N–TiO_2 has the best visible light absorption among these samples. It should be noted that there is not a definite correlation between the light absorption properties and the activity of the samples, that is, the stronger absorption of visible light dose not mean the higher decomposition rate of organic compound.

Generally, the photocatalyst activity of TiO_2 is affected by many factors such as phase composition, surface area, crystallinity, surface hydroxyl density, and oxygen vacancies. The highest photocatalytic activity of nitrogen and fluorine codoped TiO_2 here observed may be attributed to the following reasons. Firstly, the good photoactivity of N–F–TiO_2 sample is associated with its larger BET surface area and mesoporous structure. It is widely accepted that a larger surface area provides more surface activity sites for the adsorption of reactant molecules and mesoporous structure facilitates the transportation of reactant and product molecules, which making the photocatalytic process more efficient. Fig. 7b shows

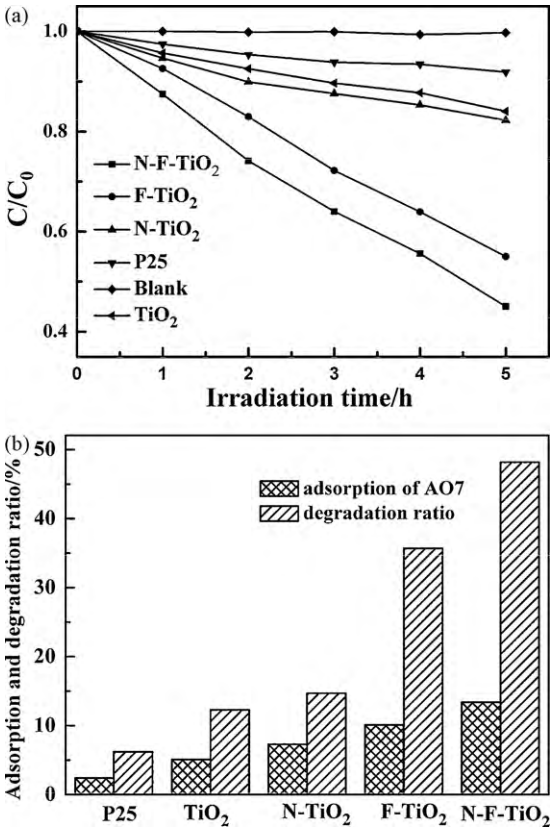

Fig. 7. (a) Photodegradation of AO7 using different samples under visible light irradiation. (b) Adsorption ratio and photodegradation ratio of AO7 over different samples.

adsorption ratio of AO7 on the surface of these samples under dark and their photodegradation ratio for AO7. The highest adsorption of AO7 on the surface of N–F–TiO_2 photocatalyst was observed. Additionally, Li et al. [22] investigated the surface acid of N–F–TiO_2 by NH_3-TPD and they found that F-doping resulted in the formation of surface acid sites. These acid sites would not only be beneficial for adsorption of reactant molecules but also act as electron acceptors. It has been reported that the photocatalytic reaction typically occurs at the surface of photocatalyst. Adsorption of reactant is generally considered to be an important factor in their photocatalytic degradation. Therefore, the unique surface characteristics of N–F–TiO_2 including a large BET surface area, mesoporous structure and surface acidity enhance the adsorption of organic compound, and thus improve the photoactivity. Secondly, it is generally recognized that the excitation electrons from the local state of N 2p to the conduct band initiate the visible photoreaction and result in the generation of conduction band electrons (e^-) and valence band holes (h^+), respectively. These charge carriers may recombine into heat without a net chemical reaction or migrate into the surface where they are trapped and eventually react with a suitable electron donor and acceptor. The electrons are captured by surface adsorbed O_2 to form superoxide radicals (O_2^-). The holes migrate to the surface and combine with OH^- adsorbed on the surface of N–TiO_2 and result in formation of $OH^\bullet$ radicals (as per Eqs. (3)–(7)). Additionally, Minero et al. [41,42] have reported that the surface modification of TiO_2 with fluoride results in the enhanced production of free $OH^\bullet$ radicals in solution by holes directly oxide water in solution (as per Eq. (8)). As the photodegradation of AO7 are largely relevant to the action of $OH^\bullet$ radicals, we propose that the enhancement of concentration of $OH^\bullet$ by F-doping would be beneficial for

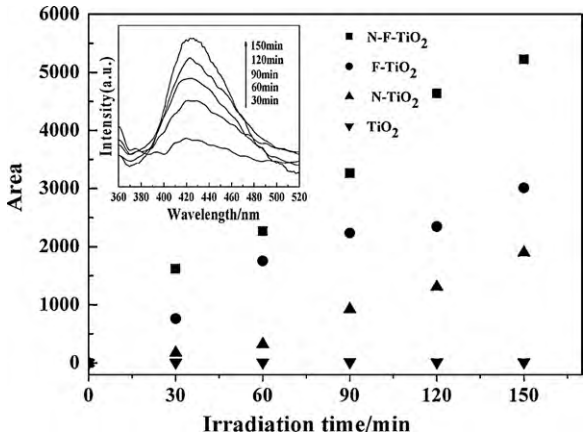

Fig. 8. Plots of the induced fluorescence peak area at 426 nm against irradiation time for terephthalic acid on different samples.

improving photocatalytic activity.

$$TiO_{2-x}N_x + h\nu \rightarrow h^+ + e^- \quad (3)$$

$$O_2 + e^- \rightarrow O_2^- \quad (4)$$

$$2O_2^- + 2H_2O \rightarrow 2H_2O_2 + O_2 \quad (5)$$

$$H_2O_2 + e^- \rightarrow {}^\bullet OH + OH^- \quad (6)$$

$$h^+ + \equiv Ti\text{–}OH^- \rightarrow \equiv Ti\text{–}{}^\bullet OH \quad (7)$$

$$\equiv Ti\text{–}F + H_2O + h^+ \rightarrow \equiv Ti\text{–}F + {}^\bullet OH_{free} + H^+ \quad (8)$$

The analysis of OH• radical's formation on these samples surface under visible light irradiation was performed by fluorescence technique with using terephthalic acid, which readily reacted with OH• radicals to produce highly fluorescent product, 2-hydroxyterephthalic acid. The intensity of the peak attributed to 2-hydroxyterephtalic acid was known to be proportional to the amount of OH• radicals formed [43]. In Fig. 8, the formation of OH• radicals on the surface of these samples is shown with time of visible light irradiation. The amounts of the produced OH• radicals increase with increasing visible irradiation time. It can be seen that the highest amount of OH• radicals are created on the surface of N–F-codoped TiO_2, the highest photoactivity among these photocatalysts is also observed. Thus, the enhancement of concentration of OH• by F and N codoping would play an important role in improving photocatalytic activity.

In summary, the higher visible photocatalytic activity of N–F–TiO_2 microsphere is ascribed to its large surface area, mesoporous structure and a synergetic effect of N and F codoping.

4. Conclusions

N and F-codoped TiO_2 photocatalyst was prepared by ethanol solvothermal method using urea as a nitrogen source and ammonium fluoride as a fluorine source. The as-prepared N–F–TiO_2 shows the spherical morphology and mesoporous structure. The band gap of TiO_2 was narrowed by N substituted O into the lattice of TiO_2, which led to the absorption edge shift to the visible region. Meanwhile, F-doping could not only suppress the transformation from anatase to rutile, but also enhance the formation of oxygen vacancies as well as OH• radicals in solution to reduce the combination of photoexcited electrons and holes. The synergetic effect of nitrogen and fluorine doped is responsible for enhancement of photodegradation activity of AO7 under irradiation of visible light.

Acknowledgments

This work has been supported by National Nature Science Foundation of China (20773039, 20977030), National Basic Research Program of China (973 Program, 2007CB613301, 2010CB732306), Science and Technology Commission of Shanghai Municipality (10520709900) and the Fundamental Research Funds for the Central Universities.

References

[1] A. Fujishima, T.N. Rao, D.A. Tryk, Titanium dioxide photocatalysis, J. Photochem. Photobiol. C 1 (2000) 1–21.
[2] M.R. Hoffmann, S.T. Martin, W. Choi, D.W. Bahnemann, Environmental applications of semiconductor photocatalysis, Chem. Rev. 95 (1995) 69–96.
[3] X.B. Chen, S.S. Mao, Titanium dioxide nanomaterials: synthesis, properties, modifications, and applications, Chem. Rev. 107 (2007) 2891–2959.
[4] R. Asahi, T. Morikawa, T. Ohwaki, K. Aoki, Y. Taga, Visible-light photocatalysis in nitrogen-doped titanium oxides, Science 293 (2001) 269–271.
[5] S. Sakthivel, H. Kisch, Daylight photocatalysis by carbon-modified titanium dioxide, Angew. Chem. Int. Ed. 42 (2003) 4908–4911.
[6] T. Ohno, M. Akiyoshi, T. Umebayashi, K. Asai, T. Mitsui, M. Matsumura, Preparation of S-doped TiO_2 photocatalysts and their photocatalytic activities under visible light, Appl. Catal. A 265 (2004) 115–121.
[7] W. Zhao, W. Ma, C. Chen, J. Zhao, Z. Shuai, Efficient degradation of toxic organic pollutants with $Ni_2O_3/TiO_{2-x}B_x$ under visible irradiation, J. Am. Chem. Soc. 126 (2004) 4782–4783.
[8] J.C. Yu, J.G. Yu, W.K. Ho, Z.T. Jiang, L.Z. Zhang, Effects of F^- doping on the photocatalytic activity and microstructures of nanocrystalline TiO_2 powders, Chem. Mater. 14 (2002) 3808–3816.
[9] H. Irie, Y. Watanabe, K. Hashimoto, Nitrogen-concentration dependence on photocatalytic activity of $TiO_{2-x}N_x$ powders, J. Phys. Chem. B 107 (2003) 5483–5486.
[10] R. Nakamura, T. Tanaka, Y. Nakato, Mechanism for visible light responses in anodic photocurrents at N-doped TiO_2 film electrodes, J. Phys. Chem. B 108 (2004) 10617–10620.
[11] M. Kitano, K. Funatsu, M. Matsuoka, M. Ueshima, M. Anpo, Preparation of nitrogen-substituted TiO_2 thin film photocatalysts by the radio frequency magnetron sputtering deposition method and their photocatalytic reactivity under visible light irradiation, J. Phys. Chem. B 110 (2006) 25266–25272.
[12] H. Irie, S. Washizuka, N. Yoshinob, K. Hashimoto, Visible-light induced hydrophilicity on nitrogen-substituted titanium dioxide films, Chem. Commun. 11 (2003) 1298–1299.
[13] C. Burda, Y. Lou, X. Chen, A.C.S. Samia, J. Stout, J.L. Gole, Enhanced nitrogen doping in TiO_2 nanoparticles, Nano Lett. 3 (2003) 1049–1051.
[14] S. Sakthivel, M. Janczarek, H. Kisch, Visible light activity and photoelectrochemical properties of nitrogen-doped TiO_2, J. Phys. Chem. B 108 (2004) 19384–19387.
[15] Y. Cong, J.L. Zhang, F. Chen, M. Anpo, Synthesis and characterization of nitrogen-doped TiO_2 nanophotocatalyst with high visible light activity, J. Phys. Chem. C 111 (2007) 6976–6982.
[16] J. Li, J. Xu, W. Dai, H. Li, K. Fan, One-pot synthesis of twist-like helix tungsten–nitrogen-codoped titania photocatalysts with highly improved visible light activity in the abatement of phenol, Appl. Catal. B 82 (2008) 233–243.
[17] Y.W. Sakai, K. Obata, K. Hashimoto, H. Irie, Enhancement of visible light-induced hydrophilicity on nitrogen and sulfur-codoped TiO_2 thin films, Vacuum 83 (2008) 683–687.
[18] Y. Cong, F. Chen, J.L. Zhang, M. Anpo, Carbon and nitrogen-codoped TiO_2 with high visible light photocatalytic activity, Chem. Lett. 35 (2006) 800–801.
[19] S. Zhang, L. Song, Preparation of visible-light-active carbon and nitrogen codoped titanium dioxide photocatalysts with the assistance of aniline, Catal. Commun. 10 (2009) 1725–1729.
[20] S. In, A. Orlov, R. Berg, F. Garciĭa, S.P. Jimenez, M.S. Tikhov, D.S. Wright, R.M. Lambert, Effective visible light-activated B-doped and B, N codoped TiO_2 photocatalysts, J. Am. Chem. Soc. 129 (2007) 13790–13791.
[21] V. Gombac, L. De Rogatis, A. Gasparotto, G. Vicario, T. Montini, D. Barreca, G. Balducci, P. Fornasiero, E. Tondello, M. Graziani, TiO_2 nanopowders doped with boron and nitrogen for photocatalytic applications, Chem. Phys. 339 (2007) 111–123.
[22] D. Li, H. Haneda, S. Hishita, N. Ohashi, Visible-light-driven N–F-codoped TiO_2 photocatalysts. 2. Optical characterization, photocatalysis, and potential application to air purification, Chem. Mater. 17 (2005) 2596–2602.
[23] D. Li, H. Haneda, S. Hishita, N. Ohashi, Visible-light-driven N–F-codoped TiO_2 photocatalysts. 1. Synthesis by spray pyrolysis and surface characterization, Chem. Mater. 17 (2005) 2588–2595.
[24] D. Huang, S. Liao, J. Liu, Z. Dang, L. Petrik, Preparation of visible-light responsive N–F-codoped TiO_2 photocatalyst by a sol–gel-solvothermal method, J. Photochem. Photobiol. A 184 (2006) 282–288.
[25] Y. Xie, Y. Li, X. Zhao, Low-temperature preparation and visible-light-induced catalytic activity of anatase F–N-codoped TiO_2, J. Mol. Catal. A 277 (2007) 119–126.
[26] S. Livraghi, K. Elghniji, A.M. Czoska, M.C. Paganini, E. Giamello, M. Ksibi, Nitrogen-doped and nitrogen–fluorine-codoped titanium dioxide. Nature and

concentration of the photoactive species and their role in determining the photocatalytic activity under visible light, J. Photochem. Photobiol. A 205 (2009) 93–97.
[27] C. Di Valentin, E. Finazzi, G. Pacchioni, Density functional theory and electron paramagnetic resonance study on the effect of N–F codoping of TiO_2, Chem. Mater. 20 (2008) 3706–3714.
[28] T. Hirakawa, Y. Nosaka, Properties of $O_2^{\bullet-}$ and $OH^{\bullet}$ formed in TiO_2 aqueous suspensions by photocatalytic reaction and the influence of H_2O_2 and some ions, Langmuir 18 (2002) 3247–3254.
[29] C.W. Guo, Y. Cao, S.H. Xie, W.L. Dai, K.N. Fan, Fabrication of mesoporous core–shell structured titania microspheres with hollow interiors, Chem. Commun. 6 (2003) 700–701.
[30] S.J. Gregg, K.S.W. Sing, Adsorption, Surface Area Porosity, Academic Press, London, 1997, p. 111.
[31] J. Tauc, Absorption edge and internal electric fields in amorphous semiconductors, Mater. Res. Bull. 5 (1970) 721–729.
[32] T. Yamaki, T. Umebayashi, T. Sumita, S. Yamamoto, M. Maekawa, A. Kawasuso, H. Itoh, Fluorine-doping in titanium dioxide by ion implantation technique, Nucl. Instrum. Methods Phys. Res. B 206 (2003) 254–258.
[33] Z. Lin, A. Orlov, R.M. Lambert, M.C. Payne, New insights into the origin of visible light photocatalytic activity of nitrogen-doped and oxygen-deficient anatase TiO_2, J. Phys. Chem. B 109 (2005) 20948–20952.
[34] I.N. Martyanov, S. Uma, S. Rodrigues, K.J. Klabunde, Structural defects cause TiO_2-based photocatalysts to be active in visible light, Chem. Commun. 21 (2004) 2476–2477.
[35] N. Serpone, Is the band gap of pristine TiO_2 narrowed by anion- and cation-doping of titanium dioxide in second-generation photocatalysts, J. Phys. Chem. B 110 (2006) 24287–24293.
[36] V.N. Kuznetsov, N. Serpone, On the origin of the spectral bands in the visible absorption spectra of visible-light-active tio$_2$ specimens analysis and assignments, J. Phys. Chem. C 113 (2009) 15110–15123.
[37] M. Sathishi, B. Viswanathan, R.P. Viswanath, C.S. Gopinath, Synthesis, characterization, electronic structure, and photocatalytic activity of nitrogen-doped TiO_2 nanocatalyst, Chem. Mater. 17 (2005) 6349–6353.
[38] X. Chen, C. Burda, Photoelectron spectroscopic investigation of nitrogen-doped titania nanoparticles, J. Phys. Chem. B 108 (2004) 15446–15449.
[39] J.F. Zhu, Z.G. Deng, F. Chen, J.L. Zhang, H.J. Chen, M. Anpo, J.Z. Huang, L.Z. Zhang, Hydrothermal doping method for preparation of Cr^{3+}–TiO_2 photocatalysts with concentration gradient distribution of Cr^{3+}, Appl. Catal. B 62 (2006) 329–335.
[40] K. Nagaveni, M.S. Hegde, G. Madras, Structure, photocatalytic activity of $Ti_{1-x}M_xO_{2\pm\delta}$ (M = W, V, Ce, Zr, Fe, and Cu) synthesized by solution combustion method, J. Phys. Chem. B 108 (2004) 20204–20212.
[41] C. Minero, G. Mariella, V. Maurino, E. Pelizzetti, Photocatalytic transformation of organic compounds in the presence of inorganic anions. 1. Hydroxyl-mediated and direct electron-transfer reactions of phenol on a titanium dioxide–fluoride system, Langmuir 16 (2000) 2632–2641.
[42] C. Minero, G. Mariella, V. Maurino, D. Vione, E. Pelizzetti, Photocatalytic transformation of organic compounds in the presence of inorganic ions. 2. Competitive reactions of phenol and alcohols on a titanium dioxide–fluoride system, Langmuir 16 (2000) 8964–8972.
[43] K. Ishibashi, A. Fujishima, T. Watanabe, K. Hashimoto, Quantum yields of active oxidative species formed on TiO_2 photocatalyst, J. Photochem. Photobiol. A 134 (2000) 139–142.